MST1 functions as a key modulator of neurodegeneration in a mouse model of ALS

Jae Keun Lee[a], Jin Hee Shin[b], Sang Gil Hwang[a], Byoung Joo Gwag[b], Ann C. McKee[c], Junghee Lee[c], Neil W. Kowall[c], Hoon Ryu[c], Dae-Sik Lim[d], and Eui-Ju Choi[a,e,1]

[a]Laboratory of Cell Death and Human Diseases, School of Life Sciences and Biotechnology, Korea University, Seoul 136-701, Korea; [b]GNT Pharma, Suwon 446-906, Korea; [c]Department of Neurology and Pathology, Boston University School of Medicine and VA Boston Healthcare System, Boston, MA 02130; [d]Department of Biological Sciences, Biomedical Research Center, Korea Advanced Institute of Science and Technology, Daejon 305-701, Korea; and [e]College of Pharmacy, Korea University, Yeongi, Chungnam 339-700, Korea

Edited by Jeffrey D. Rothstein, Johns Hopkins University, Baltimore, MD, and accepted by the Editorial Board June 1, 2013 (received for review January 15, 2013)

Amyotrophic lateral sclerosis (ALS) is an adult-onset neurodegenerative disorder characterized by loss of motor neurons. Dominant mutations in the gene for superoxide dismutase 1 (SOD1) give rise to familial ALS by an unknown mechanism. Here we show that genetic deficiency of mammalian sterile 20-like kinase 1 (MST1) delays disease onset and extends survival in mice expressing the ALS-associated G93A mutant of human SOD1. SOD1(G93A) induces dissociation of MST1 from a redox protein thioredoxin-1 and promotes MST1 activation in spinal cord neurons in a reactive oxygen species–dependent manner. Moreover, MST1 was found to mediate SOD1(G93A)-induced activation of p38 mitogen-activated protein kinase and caspases as well as impairment of autophagy in spinal cord motoneurons of SOD1(G93A) mice. Our findings implicate MST1 as a key determinant of neurodegeneration in ALS.

neurotoxicity | ROS

Amyotrophic lateral sclerosis (ALS) is an adult-onset neurodegenerative disorder characterized by the selective loss of motor neurons in the brain and spinal cord. Whereas most cases (~90%) of ALS are sporadic (sALS), both sALS and familial ALS (fALS) share similar clinical characteristics, suggestive of common disease mechanisms. Mutations in the gene for superoxide dismutase 1 (SOD1) are one of the most common causes of fALS and give rise to disease as a result of acquired gain-of-function toxicity (1, 2). Studies using the disease-model mice overexpressing ALS-linked mutants of human SOD1 have suggested that many mutations result in oxidative damage and apoptosis in motor neurons (2, 3). The molecular mechanism by which SOD1 mutants induce neurodegeneration remains unclear, however.

Mammalian sterile 20 (STE20)-like kinase 1 (MST1) is a multifunctional serine-threonine kinase that belongs to the family of class II germinal center kinases (4–6). MST1 is composed of a catalytic domain in the amino-terminal region, an inhibitory domain in the central region, and a regulatory Salvador/Rassf/Hippo (SARAH) domain in the carboxyl-terminal region (7, 8). The SARAH domain is responsible for the homo-dimerization of MST1, which contributes to the mechanism underlying MST1 activation (7, 9). It also mediates the formation of heteromeric complexes with other SARAH domain-containing proteins such as 45 kDa WW domain protein and Rassf proteins (7, 8). MST1 is expressed ubiquitously and is associated with the regulatory mechanisms for many biological events including cell growth, apoptosis, stress response, and senescence (10, 11). In particular, MST1 has been recently suggested to mediate neuronal cell death initiated by oxidative stress (11, 12).

Given that oxidative stress contributes to the pathogenesis of ALS, we investigated the possible role of MST1 in the neurotoxicity underlying fALS with use of a transgenic mouse model.

Results and Discussion

Motor Neurons in sALS Patients and SOD1(G93A) Mice Show Higher Activity of MST1. We first examined MST1 activity in primary motor neurons (PMNs) prepared from the spinal cord of E13 embryos of control B6 mice or transgenic mice expressing wild-type (WT) or the ALS-associated G93A mutant of human SOD1. The phosphorylated (active) form of MST1 (phospho-MST1) was detected in PMNs from the SOD1(G93A) mice by immunofluorescence analysis, and this phosphorylation was abolished by exposure of the cells to scavengers of reactive oxygen species (ROS) including Trolox and *N*-acetylcysteine (NAC) (Fig. S1), suggesting that SOD1(G93A) induces MST1 activation in a manner dependent on ROS accumulation. In contrast, SOD1 (WT) did not induce MST1 activation in PMNs. Postmortem sections of the spinal cord obtained from sALS patients and neurologically normal control individuals were also examined by immunohistochemical analysis with antibodies specific for phospho-MST1. The intensity of phospho-MST1 immunostaining was greater in motor neurons of sALS patients than those of control individuals (Fig. 1*A*, Fig. S2). MST1 activity was also increased in the lumbar spinal cord in SOD1(G93A) mice before symptom onset, compared with that in control mice (Fig. 1*B*). Furthermore, immunofluorescence analysis indicated that the levels of phospho-MST1 were greater in motor neurons in the lumbar spinal cord of SOD1(G93A) mice at presymptomatic (8-wk-old) (Fig. 1*C*) and symptomatic (16-wk-old) stages (Fig. S3*A*), compared with those in control mice. Interestingly, phosphorylation (activation) of MST1 was not detected in astrocytes in the lumbar spinal cord in SOD1(G93A) mice (Fig. S3*B*), suggesting that the activation of MST1 in the ALS model mice is specific for motor neurons.

Genetic Ablation of MST1 Alleviates fALS-Like Disease Phenotype in Vivo. Next, we investigated whether MST1 might be associated with the ALS disease-related features of SOD1(G93A) mice. Homozygous deletion of *Mst1* in SOD1(G93A) mice not only delayed symptom onset (Fig. 2*A*) and mortality (Fig. 2*B*) but also improved the viability of spinal cord motor neurons (Fig. 2 *C* and *D*), implicating MST1 in ALS-associated motor neuron toxicity. Analysis of neuromuscular function with the rotarod (Fig. 2*E*), paw grip endurance (PaGE) (Fig. 2*F*), and stride-length (Fig.

Author contributions: J.K.L., J.H.S., B.J.G., and E.-J.C. designed research; J.K.L., J.H.S., and S.G.H. performed research; A.C.M., J.L., N.W.K., H.R., and D.-S.L. contributed new reagents/analytic tools; J.K.L., J.H.S., S.G.H., B.J.G., D.-S.L., and E.-J.C. analyzed data; and J.K.L. and E.-J.C. wrote the paper.

The authors declare no conflict of interest.

This article is a PNAS Direct Submission. J.D.R. is a guest editor invited by the Editorial Board.

[1]To whom correspondence should be addressed. E-mail: ejchoi@korea.ac.kr.

This article contains supporting information online at www.pnas.org/lookup/suppl/doi:10.1073/pnas.1300894110/-/DCSupplemental.

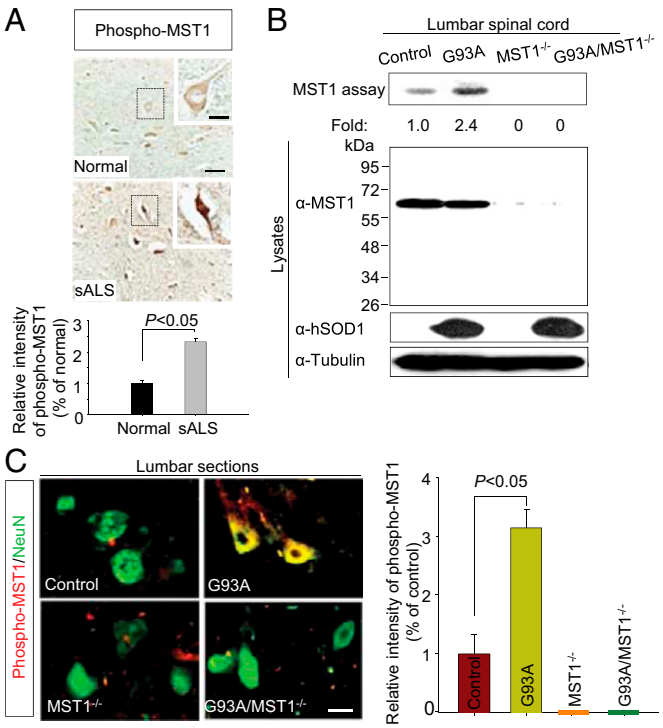

Fig. 1. sALS patients as well as SOD1(G93A) mice show higher activity of MST1 in motor neurons. (*A*) Representative immunohistochemical analysis of ventral motor neurons in postmortem spinal cord sections from a sALS patient and a control individual with antibodies to phospho-MST1 is shown (*Upper*). (Scale bar, 50 μm.) The boxed regions are shown at higher magnification in the inserts. (Scale bar, 20 μm.) The relative intensity of phospho-MST1 immunostaining quantified for all human subjects ($n = 8$ for normal, $n = 9$ for sALS) is shown (*Lower*) (Fig. S2). Quantitative data are means ± SEM. (*B*) MST1 activity in the lumbar spinal cord of 8-wk-old control, SOD1 (G93A), MST1$^{-/-}$, and SOD1(G93A)/MST1$^{-/-}$ mice was determined with immune complex kinase assay with GST–Forkhead box protein O3 (FOXO3) as substrate. Activity relative to that of control mice is indicated below each lane. Tissue lysates were also subjected to immunoblot analysis with antibodies to MST1, to human SOD1 (hSOD1), and to $\mathcal{D}$-tubulin (loading control). (*C*) Sections of the lumbar spinal cord of control, SOD1(G93A), MST1$^{-/-}$, and SOD1(G93A)/MST1$^{-/-}$ mice ($n = 4$ per group) were subjected to immunofluorescence staining with antibodies to phospho-MST1 (red) and to NeuN (green). (Scale bar, 10 μm.) The relative intensity of phospho-MST1 immunostaining quantified for all groups is shown (*Right*). Quantitative data are means ± SEM.

2*G*) tests also revealed that genetic ablation of MST1 significantly ameliorated the ALS-like phenotype of SOD1(G93A) mice. Taken together, these results suggested that MST1 might mediate the disease-related neurotoxicity in the ALS model mice.

SOD1(G93A) Induces Dissociation of MST1 from Thioredoxin-1 and Promotes MST1 Homodimerization. Next, we investigated the possible mechanism by which SOD1(G93A) induces MST1 activation. We have recently reported that a redox protein thioredoxin-1 (Trx1) inhibits ROS-induced MST1 activation in intact cells (13). Moreover, in in vitro kinase assays, Trx1 directly inhibited the kinase activity of the MST1 immunoprecipiates that had been obtained from SOD1(G93A)-expressing cells (Fig. 3*A*). With these findings, we further examined the possible role of this redox protein in the mechanism underlying activation of MST1 by SOD1 (G93A). Coimmunoprecpitation analysis revealed that MST1 physically associated with Trx1 in mouse motor-neuron-like NSC34 cells stably expressing human SOD1(WT) but not in those expressing SOD1(G93A), and this dissociation of the MST1–Trx1 complex induced by SOD1(G93A) was accompanied by an increase in MST1 activity (Fig. 3*B*). NAC and Trolox, both of which decreased intracellular levels of ROS enhanced by SOD1 (G93A) (Fig. S4), abrogated the effects of SOD1(G93A) on the MST1–Trx1 interaction and MST1 activation (Fig. 3*B*). It is also worthwhile to note that MST1 did not physically associate with either SOD1(WT) or SOD1(G93A) (Fig. S5). Consistent with these results in the transfected NSC34 cells, separate coimmunoprecipitation data showed the physical association of MST1 and Trx1 in the lumbar spinal cord of control mice and that this interaction was disrupted in the lumbar spinal cord of SOD1 (G93A) mice (Fig. 3*C*). The MST1–Trx1 interaction in the lumbar spinal cord was also examined by an in situ proximity ligation assay (PLA), which allows detection of protein–protein interactions in cells (14), with using anti-Trx1 and anti-MST1 antibodies. Again, MST1 was found to interact with Trx1 in ventral motor neurons from control mice but not in those from SOD1 (G93A) mice (Fig. S6*A*). We also confirmed the specificity of PLA signal indicating the MST1–Trx1 interaction in lumbar sections of control mice (Fig. S6*B*). As shown in Fig. S6*B*, we observed that the PLA signal was abolished when this assay was performed in the presence of MST1 or Trx1 protein to neutralize anti-MST1 or anti-Trx1 antibodies, respectively.

We next examined whether SOD1(G93A) could affect MST1 homodimerization, which contributes to MST1 activation (9), after transfecting 293T cells with plasmids encoding Myc epitope-tagged MST1 and Flag-MST1 together with plasmids for either Flag-SOD1(G93A) or Flag-SOD1. Coimmunoprecipitation data revealed that SOD1(G93A) promoted MST1 homodimerization and that this effect was blocked by ROS scavengers Trolox and NAC (Fig. 3*D*). Concomitantly, SOD1(G93A) induced dissociation of MST1 from Trx1 as well as MST1 activation in a manner sensitive to the ROS scavengers. Collectively, these results suggested that MST1 forms a complex with Trx1 under reduced conditions, and that ROS generation in SOD1(G93A)-expressing cells promotes the release of MST1 from Trx1 and thereby facilitates the homodimerization and activation of MST1.

MST1 Mediates the SOD1(G93A)-Induced Activation of p38 MAPK and Caspases. The p38 mitogen-activated protein kinase (MAPK) and caspases have been implicated in disease pathogenesis in ALS mouse models (15, 16). Given that p38 MAPK and caspases may also play a role in MST1-mediated cell death (17), we examined the activation status of p38 and caspases in the lumbar spinal cord. Activation of p38 and its upstream kinase apoptosis signal–regulated kinase 1 () was apparent in the lumbar spinal cord of 8-wk-old SOD1(G93A) mice, and this activation was abolished in SOD1(G93A)/MST1$^{-/-}$ mice (Fig. 4*A*). Cleavage (activation) of caspase-9 and caspase-3 was also detected in the lumbar spinal cord of 12-wk-old SOD1(G93A) mice but not in that of SOD1 (G93A)/MST1$^{-/-}$ mice (Fig. 4*B*). In addition, cleavage of caspase-3 was observed in lumbar spinal cord motoneurons of 12-wk-old SOD1(G93A) mice, and this cleavage was again mitigated by deletion of *Mst1* (Fig. 4*C*). Collectively, these results suggested that SOD1(G93A) induces MST1 activation, which in turn mediates activation of the p38 signaling pathway as well as that of caspase-9 and -3 in the lumbar spinal cord of ALS mice. The p38 inhibitor SB203580 blocked SOD1(G93A)-induced activation of caspase-9 and -3 in NSC34 cells (Fig. S7*A*), whereas the pan-caspase inhibitor carbobenzoxy-valyl-alanyl-aspartyl-[Omethyl]-fluoromethylketone (zVAD-fmk) did not affect p38 MAPK signaling activated by SOD1(G93A) (Fig. S7*B*), suggesting that the p38 pathway mediates SOD1(G93A)-induced caspase activation. Neither SB203580 nor zVAD–fmk affected SOD1 (G93A)-induced MST1 activation (Fig. S7), consistent with our data suggesting that MST1 acts upstream of the p38 pathway as well as of caspase-9 and -3.

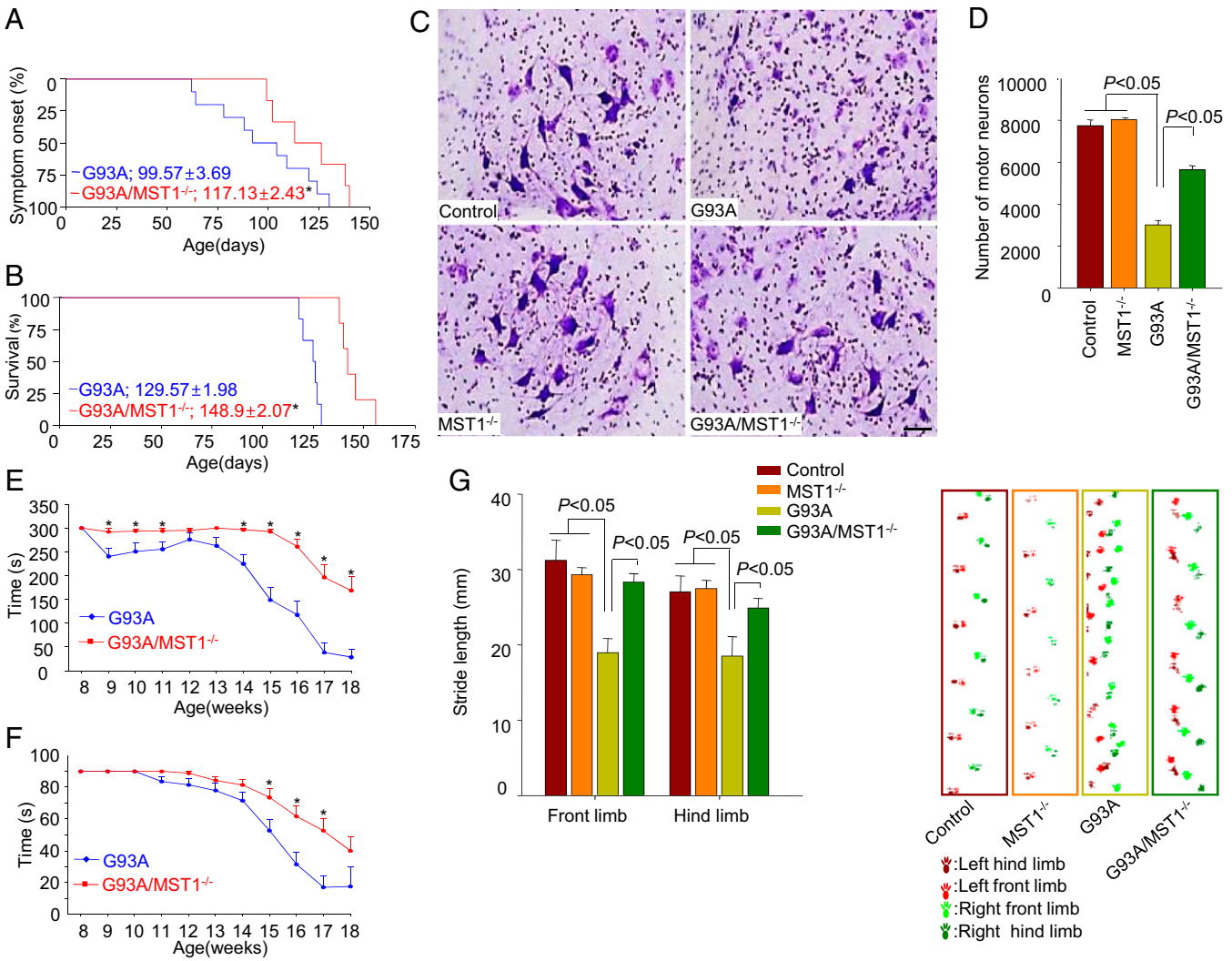

Fig. 2. MST1 deficiency ameliorates fALS disease signs. (*A* and *B*) Kaplan–Meyer analysis of the onset of rotarod deficits (*A*) and of survival (*B*) in SOD1(G93A) and SOD1(G93A)/MST1$^{-/-}$ mice ($n = 21$). The mean ± SEM values for age at 50% change for each group are indicated. *$P < 0.05$ versus SOD1(G93A). (*C*) Cresyl violet-stained sections of the ventral lumbar spinal cord from 16-wk-old mice of the indicated genotypes. (Scale bar, 20 μm.) (*D*) Stereological assessment of viability of motor neurons. Numbers of viable motor neurons were measured by counting the Cresyl violet-stained large neurons in the lumbar spinal cord of 16-wk-old control ($n = 5$), MST1$^{-/-}$ ($n = 4$), SOD1(G93A) ($n = 5$), and SOD1(G93A)/MST1$^{-/-}$ ($n = 5$) mice. (*E* and *F*) Motor function of SOD1(G93A) and SOD1 (G93A)/MST1$^{-/-}$ mice ($n = 21$) was examined with the rotarod (*E*) and PaGE (*F*) tests. *$P < 0.05$ versus SOD1(G93A). (G) Stride-length analysis of 14-wk-old mice of the indicated genotypes ($n = 21$). Representative raw stride-length data are shown (*Right*). Quantitative data in *D*–*G* are means ± SEM.

MST1 Mediates the SOD1(G93A)-Induced Abnormality in Autophagic Flux. Defects in autophagy are thought to give rise to neurodegeneration (18), with failure of this process having been shown to contribute to the pathogenesis of ALS in clinical and experimental studies (19, 20). Expression of SOD1(G93A) increased the amounts of autophagy markers including beclin-1 [autophagy related 6 homolog (ATG6)], microtubule-associated protein 1 light chain 3 (LC3), and the ATG5–ATG12 complex in NSC34 cells, compared with those apparent in cells expressing human SOD1(WT) (Fig. S8*A*). The effects of SOD1(G93A) on the autophagy markers were inhibited by treatment of the cells with SB203580, but not by that with zVAD–fmk. Beclin-1 plays an important role in the early stage of autophagy (21), and LC3-II and the ATG12–ATG5 complex are protein markers for autophagosome formation (22). These findings prompted us to examine whether MST1 mediates the effect of SOD1(G93A) on the autophagy markers in motor neurons. We introduced green fluorescence protein (GFP)-tagged LC3 into PMNs and monitored the cells for the presence of punctate GFP–LC3 fluorescence, indicative of recruitment of the tagged protein to autophagosome membranes (23). The intensity of punctuate GFP–LC3 fluorescence was greatly increased in SOD1(G93A) PMNs compared with control PMNs, and this increase was markedly attenuated by SB203580, but not by zVAD–fmk (Fig. S8*B*). Importantly, genetic deficiency of MST1 also attenuated the SOD1(G93A)-dependent increase in GFP–LC3–labeled autophagosomes in PMNs (Fig. S8*C*). Consistent with these findings, the abundance of autophagy markers (beclin-1, LC3-II, ATG5–ATG12) in the lumbar spinal cord was increased in 16-wk-old SOD1(G93A) transgenic mice compared with age-matched control mice, and this increase was abolished by genetic ablation of MST1 (Fig. 5*A*). Electron microscopy also revealed that the number of autophagosomes, defined as double-membrane vesicles, in ventral motor neurons of the lumbar spinal cord was increased in SOD1(G93A) mice compared with control mice, and again this effect of SOD1(G93A) was attenuated by genetic ablation of MST1 (Fig. 5*B*). We also found that p62, a target protein for autophagy-dependent degradation (24),

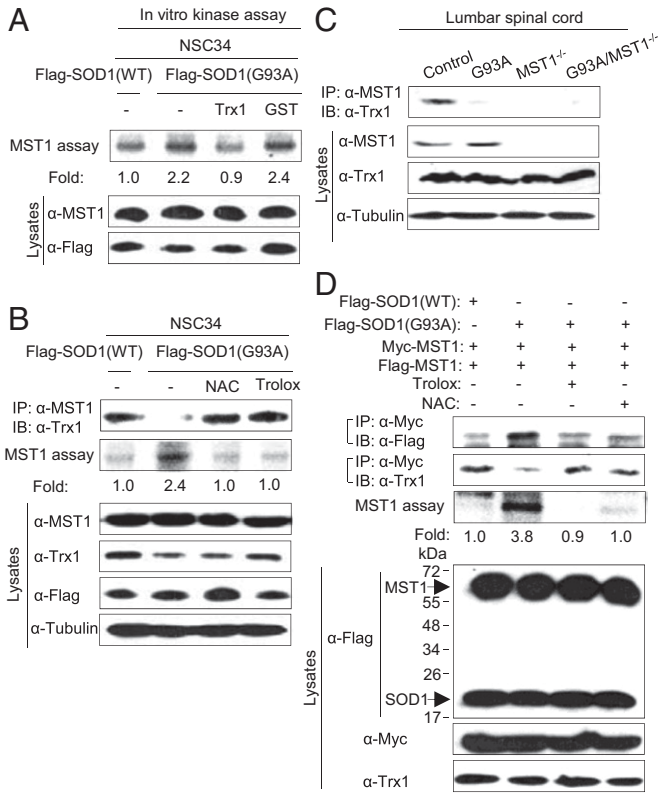

Fig. 3. SOD1(G93A) induces dissociation of MST1 from Trx1 and promotes the homodimerization and activation of MST1. (*A*) Lysates of NSC34 cells stably expressing Flag-tagged human SOD1(WT) or SOD1(G93A) were subjected to immunoprecipitation with antibodies to MST1. The resulting MST1 precipitates were incubated at 30 °C for 30 min in 20 μL of kinase reaction buffer in the absence or presence of 2 μg Trx1 or GST and were then examined for MST1 activity with GST–FOXO3 as substrate. (*B*) NSC34 cells stably expressing Flag-tagged human SOD1(WT) or SOD1(G93A) were incubated in the absence or presence of 100 μM Trolox or 3 mM NAC for 12 h, lysed, and subjected to immunoprecipitation (IP) with antibodies to MST1. The resulting precipitates were analyzed by immunoblot analysis (IB) with antibodies to Trx1 and were assayed for MST1 activity with GST–FOXO3 as substrate. Cell lysates were also examined directly by immunoblot analysis with antibodies to MST1, to Trx1, to Flag, or to $\mathcal{D}$-tubulin. (*C*) Coimmunoprecipitation analysis showing the interaction between MST1 and Trx1 in the lumbar spinal cord of 8-wk-old mice with the indicated genotypes ($n = 3$). Tissue lysates were also examined by immunoblot analysis with antibodies to MST1, to Trx1, and to α-tubulin. (*D*) 293T cells transfected for 48 h with the indicated combinations of plasmids encoding Flag-tagged SOD1(WT), Flag-SOD1(G93A), and Flag-tagged or Myc epitope–tagged MST1 were incubated in the absence or presence of 100 μM Trolox or 3 mM NAC for 12 h, lysed, and subjected to immunoprecipitation with antibodies to Myc. The resulting precipitates were subjected to immunoblot analysis with antibodies to Flag and to Trx1 and were assayed for MST1 activity with GST–FOXO3 as substrate. Cell lysates were also examined directly by immunoblot analysis with antibodies to Flag, to Myc, and to Trx1.

accumulated in lumbar spinal cord motoneurons of SOD1(G93A) mice (Fig. 5*A*, Fig. S9), indicative of a defect in autophagic flux (that is, in the balance between induction of autophagy and autophagic degradation). This accumulation of p62 was attenuated by genetic ablation of MST1, suggesting that MST1 is responsible for the abnormality in autophagic flux in lumbar spinal cord motoneurons of SOD1(G93A) mice.

In this study, we have shown that MST1 activity was increased presymptomatically in motor neurons, but not in glial cells, of the spinal cord in SOD1(G93A) mice and that deficiency of the MST1 gene improved the severity of disease manifestations in the fALS model mice. Furthermore, our data with ROS scavengers suggest that intracellular ROS mediates the SOD1(G93A)-induced activation of MST1, although the origin of ROS generation induced by SOD1(G93A) remains unclear (25). We also found that Trx1 physically associates with MST1 in a basal state, and that SOD1(G93A) induces dissociation of the MST1–Trx1 complex in a ROS-dependent manner and thereby promotes the homodimerization of MST1, which is an integral part of the mechanism for the activation of MST1 (9). Several possible mechanisms may be proposed for the ROS-dependent release of MST1 from Trx1. One possibility would be that only the reduced form of Trx1 binds MST1, and that the oxidation of Trx1 expedites the dissociation of the MST1–Trx1 complex. Alternatively, MST1 may be targeted by ROS-mediated reaction(s), and the oxidized form of MST1 may be released from Trx1. Aside from these possibilities, our results suggest that Trx1 functions as a negative regulator of the ROS-induced activation of MST1 in SOD1(G93A) mice. Additionally, given that oxidative stress is implicated in both sporadic and fALS

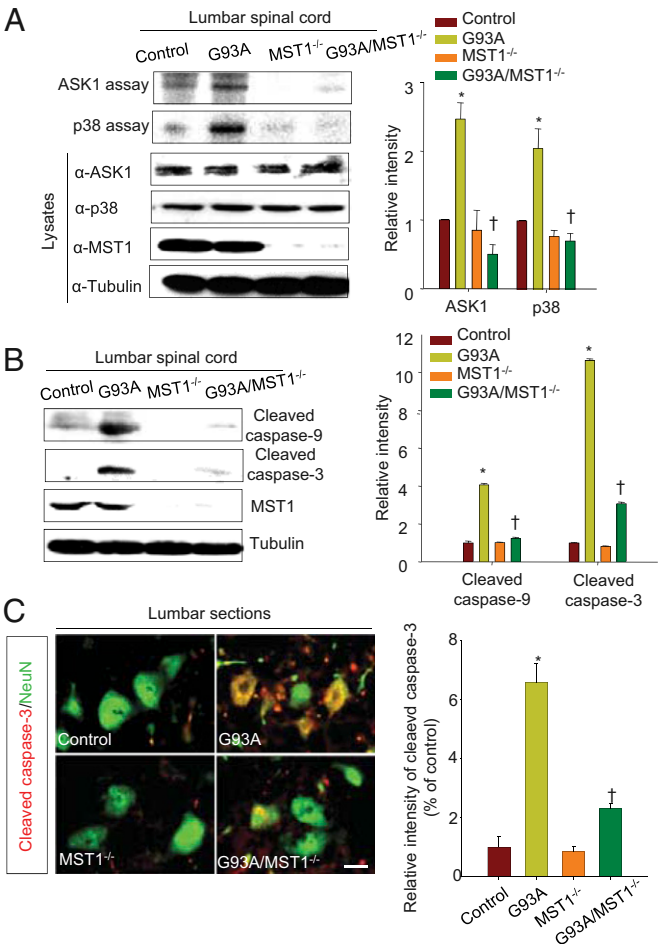

Fig. 4. MST1 mediates SOD1(G93A)-induced activation of p38 MAPK and caspases. (*A*) ASK1 and p38 activities in the lumbar spinal cord of 8-wk-old mice of the indicated genotypes were determined with immune complex kinase assays (*Left*) and quantified by densitometry (*Right*; $n = 3$). (*B*) Representative immunoblot analysis of the cleaved forms of caspase-9 and caspase-3 in the lumbar spinal cord of 12-wk-old mice (*Left*) and densitometric analysis of immunoblot bands (*Right*; $n = 4$). (*C*) Sections of the lumbar spinal cord of 12-wk-old control, SOD1(G93A), MST1$^{-/-}$, and SOD1(G93A)/MST1$^{-/-}$ mice ($n = 4$ per group) were subjected to immunofluorescence staining with antibodies to cleaved caspase-3 (red) and to neuronal nuclei (NeuN) protein (green) (*Left*). (Scale bar, 10 μm.) The relative intensity of cleaved caspase-3 immunostaining quantified for all groups is shown (*Right*). Quantitative data are means ± SEM *$P < 0.05$ versus control, †$P < 0.05$ versus SOD1(G93A).

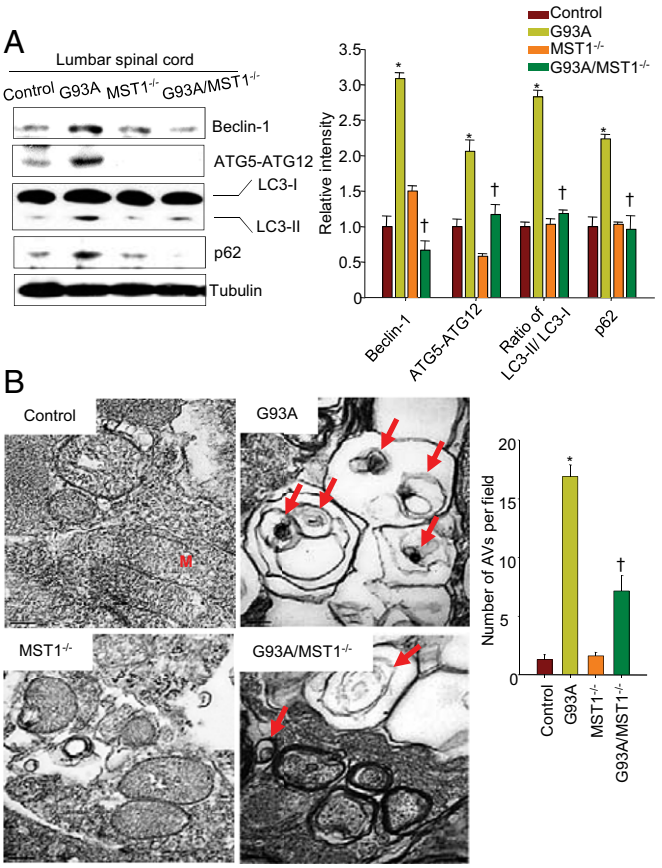

Fig. 5. MST1 mediates SOD1(G93A)-induced autophagosome accumulation. (*A*) Representative immunoblot analysis of autophagy markers in the lumbar spinal cord of 16-wk-old mice (*Left*) and densitometric analysis of immunoblot bands (*Right*; $n = 4$). (*B*) Electron microscopy of double-membrane autophagy vacuoles (AVs, arrows) in ventral motor neurons of the lumbar spinal cord of 16-wk-old mice (*Left*). M, mitochondria. (Scale bar, 200 nm.) The number of AVs in motor neurons was also determined (*Right*, $n = 3$). All quantitative data are means ± SEM $^*P < 0.05$ versus control, $^{\dagger}P < 0.05$ versus SOD1(G93A).

cases (26–28), ROS generation might be the common mechanism for MST1 activation in ALS.

The activation of MST1 by SOD1(G93A) results in the stimulation of p38 MAPK and caspase-9 and -3 as well as in autophagosome accumulation due to autophagic imbalance, all of which contribute to the demise of motor neurons both in vitro and in vivo. The p38 MAPK pathway appears to mediate both caspase activation and the impairment in autophagic flux in parallel in SOD1(G93A)-expressing motor neurons. Collectively, our findings implicate MST1 as a key mediator of the ALS-associated neurodegeneration, and they therefore identify it as a potential therapeutic target for ALS as well as other motor neuron diseases.

Materials and Methods

A detailed description of the materials and methods can be seen in *SI Materials and Methods*.

Animal Models and Breeding Schemes. MST1 knockout mice were described previously (29). ALS model mice expressing human SOD1(G93A) (B6SJL–Tg [SOD1–G93A]1Gur/J) and mice expressing human SOD1(WT) (B6SJL–Tg [SOD1]2Gur/J) were obtained from the Jackson Laboratory. SOD1(G93A) transgenic mice on the MST1$^{-/-}$ background were generated according to the following breeding scheme: SOD1(G93A) males were mated with MST1$^{+/-}$ females, and the resulting SOD1(G93A)/MST1$^{+/-}$ F_1 males were then mated with MST1$^{+/-}$ females to yield all of the genotypes studied. Genotyping of littermates was performed with standard PCR-based protocols and primer sets described previously (29, 30). All animal procedures were approved by the Institutional Animal Care and Use Committee of Korea University.

Behavioral Assessments. Mice were analyzed for motor dysfunction with the rotarod, PaGE, and stride-length tests beginning at 8 wk of age. Behavioral analysis with a rotarod instrument (Columbus Instruments) was performed twice a week until each mouse was no longer able to perform the task. Each animal was subjected to three trials at 16 rpm. A cutoff time point was set arbitrarily at 300 s, and a mouse remaining on the rotarod for this time was considered to be asymptomatic. The onset of disease symptoms was determined as the first day when a mouse showed motor dysfunction in rotarod performance. The average performance duration up to the cutoff time was recorded for each mouse and used for analysis. The PaGE test was used to evaluate grip strength and performed twice a week. The time during which a mouse remained attached to the inverted lid with both hind limbs was measured. Each mouse was allowed three attempts to hold onto the inverted lid for an arbitrary maximum of 90 s, and the longest time was recorded. To evaluate motor coordination, we analyzed stride length for 14-wk-old mice with the use of a CatWalk apparatus (Noldus) (31). Each mouse was placed individually on the CatWalk walkway and allowed to traverse the glass plate of the walkway as many times as needed to obtain at least three fluent crossings in the dark. Where the mouse paws were placed on the glass plate, light was reflected down and the illuminated contact areas were recorded with a charge-coupled device camera underneath the glass plate. Contact areas were indexed automatically and assigned to the respective colored paws, which allowed quantitative analysis of gait with the use of CatWalk software 7.1. The mean value for stride length was calculated for at least 10 consecutive strides.

Statistical Analysis. Data are presented as means ± SEM. Comparisons between two groups were performed with the independent-samples *t* test, and those among more than two groups were performed with analysis of variance (ANOVA) followed by the Student Newman–Keuls test. Data for symptom onset and survival were subjected to Kaplan–Meier analysis. All analyses were performed with SPSS version 12.0 software for Windows. A *P* value of < 0.05 was considered statistically significant.

ACKNOWLEDGMENTS. We thank S. Kang (Korea University) for providing Flag-SOD1 and Flag-SOD1(G93A) cDNAs. This work was supported by Grant 351-2009-1-E00030 (to J.K.L) and by National Research Foundation Grants 2006-0093855, and 2011-0030141, and 2009-0081488 funded by the Ministry of Science, ICT & Future Planning of Korea (to E.-J.C.). J.K.L was supported by a Korea University grant. J.L. and N.W.K. were supported by Veterans Affairs Merit Award.

1. Gurney ME, et al. (1994) Motor neuron degeneration in mice that express a human Cu,Zn superoxide dismutase mutation. *Science* 264(5166):1772–1775.
2. Cleveland DW, Rothstein JD (2001) From Charcot to Lou Gehrig: Deciphering selective motor neuron death in ALS. *Nat Rev Neurosci* 2(11):806–819.
3. Pasinelli P, Brown RH (2006) Molecular biology of amyotrophic lateral sclerosis: Insights from genetics. *Nat Rev Neurosci* 7(9):710–723.
4. Creasy CL, Chernoff J (1995) Cloning and characterization of a human protein kinase with homology to Ste20. *J Biol Chem* 270(37):21695–21700.
5. Dan I, Watanabe NM, Kusumi A (2001) The Ste20 group kinases as regulators of MAP kinase cascades. *Trends Cell Biol* 11(5):220–230.
6. Taylor LK, Wang HC, Erikson RL (1996) Newly identified stress-responsive protein kinases, Krs-1 and Krs-2. *Proc Natl Acad Sci USA* 93(19):10099–10104.
7. Creasy CL, Ambrose DM, Chernoff J (1996) The Ste20-like protein kinase, Mst1, dimerizes and contains an inhibitory domain. *J Biol Chem* 271(35):21049–21053.
8. Scheel H, Hofmann K (2003) A novel interaction motif, SARAH, connects three classes of tumor suppressor. *Curr Biol* 13(23):R899–R900.
9. Glantschnig H, Rodan GA, Reszka AA (2002) Mapping of MST1 kinase sites of phosphorylation. Activation and autophosphorylation. *J Biol Chem* 277(45):42987–42996.
10. de Souza PM, Lindsay MA (2004) Mammalian Sterile20-like kinase 1 and the regulation of apoptosis. *Biochem Soc Trans* 32(Pt3):485–488.
11. Lehtinen MK, et al. (2006) A conserved MST-FOXO signaling pathway mediates oxidative-stress responses and extends life span. *Cell* 125(5):987–1001.
12. Yuan Z, et al. (2009) Regulation of neuronal cell death by MST1-FOXO1 signaling. *J Biol Chem* 284(17):11285–11292.
13. Chae JS, Gil Hwang S, Lim DS, Choi EJ (2012) Thioredoxin-1 functions as a molecular switch regulating the oxidative stress-induced activation of MST1. *Free Radic Biol Med* 53(12):2335–2343.
14. Söderberg O, et al. (2008) Characterizing proteins and their interactions in cells and tissues using the in situ proximity ligation assay. *Methods* 45(3):227–232.
15. Dewil M, dela Cruz VF, Van Den Bosch L, Robberecht W (2007) Inhibition of p38 mitogen activated protein kinase activation and mutant SOD1(G93A)-induced motor neuron death. *Neurobiol Dis* 26(2):332–341.

16. Li M, et al. (2000) Functional role of caspase-1 and caspase-3 in an ALS transgenic mouse model. *Science* 288(5464):335–339.
17. Graves JD, et al. (1998) Caspase-mediated activation and induction of apoptosis by the mammalian Ste20-like kinase Mst1. *EMBO J* 17(8):2224–2234.
18. Hara T, et al. (2006) Suppression of basal autophagy in neural cells causes neurodegenerative disease in mice. *Nature* 441(7095):885–889.
19. Hetz C, et al. (2009) XBP-1 deficiency in the nervous system protects against amyotrophic lateral sclerosis by increasing autophagy. *Genes Dev* 23(19):2294–2306.
20. Sasaki S (2011) Autophagy in spinal cord motor neurons in sporadic amyotrophic lateral sclerosis. *J Neuropathol Exp Neurol* 70(5):349–359.
21. Levine B, Klionsky DJ (2004) Development by self-digestion: Molecular mechanisms and biological functions of autophagy. *Dev Cell* 6(4):463–477.
22. Kabeya Y, et al. (2000) LC3, a mammalian homologue of yeast Apg8p, is localized in autophagosome membranes after processing. *EMBO J* 19(21):5720–5728.
23. Klionsky DJ, et al. (2008) Guidelines for the use and interpretation of assays for monitoring autophagy in higher eukaryotes. *Autophagy* 4(2):151–175.
24. Bjørkøy G, et al. (2005) p62/SQSTM1 forms protein aggregates degraded by autophagy and has a protective effect on huntingtin-induced cell death. *J Cell Biol* 171(4):603–614.
25. Turner BJ, Talbot K (2008) Transgenics, toxicity and therapeutics in rodent models of mutant SOD1-mediated familial ALS. *Prog Neurobiol* 85(1):94–134.
26. Beal MF, et al. (1997) Increased 3-nitrotyrosine in both sporadic and familial amyotrophic lateral sclerosis. *Ann Neurol* 42(4):644–654.
27. Bogdanov M, et al. (2000) Increased oxidative damage to DNA in ALS patients. *Free Radic Biol Med* 29(7):652–658.
28. Ferrante RJ, et al. (1997) Evidence of increased oxidative damage in both sporadic and familial amyotrophic lateral sclerosis. *J Neurochem* 69(5):2064–2074.
29. Oh S, et al. (2009) Crucial role for Mst1 and Mst2 kinases in early embryonic development of the mouse. *Mol Cell Biol* 29(23):6309–6320.
30. Shin JH, et al. (2007) Concurrent administration of Neu2000 and lithium produces marked improvement of motor neuron survival, motor function, and mortality in a mouse model of amyotrophic lateral sclerosis. *Mol Pharmacol* 71(4):965–975.
31. Vandeputte C, et al. (2010) Automated quantitative gait analysis in animal models of movement disorders. *BMC Neurosci* 11:92.